

# Widely Wavelength-tunable Mode-locked Fiber Laser Based on a 45° Tilted Fiber Grating and Polarization Maintaining Fiber

Bingbing Lu, Chuanhang Zou, Qianqian Huang, Zhijun Yan, Zhikun Xing, Mohammed Al Araimi, Aleksey Rozhin, Kaiming Zhou, Lin Zhang, and Chengbo Mou

**Abstract**—We present a passively mode-locked Erbium-doped fiber laser with tunable parameters including central wavelength, 3dB bandwidth and pulse duration. The mode-locking mechanism of the laser is realized by using single-walled carbon nanotubes polyvinyl alcohol (SWCNTs-PVA) composite film as saturable absorber. The tunable operation is implemented via a fiber birefringence filter consisting of a polarization maintaining (PM) fiber and a Brewster fiber grating. The laser achieves a maximum spectral tuning range of 36 nm with 8 cm PM fiber. The maximum spectral width variation of 5.19 nm is acquired when the PM fiber is 12 cm. Simultaneously, the spectral widths of pulses at different central wavelengths are also adjustable. Furthermore, the total cavity length is 8.28 m, which is the shortest cavity length to obtain such wide tuning range in an Erbium-doped fiber laser based on SWCNTs.

**Index Terms**—Passively mode-locked fiber laser, spectral width, pulse width, tilted fiber grating, wavelength-tunable.

## I. INTRODUCTION

WAVELENGTH-TUNABLE mode-locked fiber lasers have appealed to enormous interest of researchers owing to their highly potential applications in wide domains such as spectroscopy, optical communications, fiber-optic sensors, biomedical research [1]-[3]. The passively mode-locked fiber laser has many advantages such as compactness, alignment-free structure, and cost-effectiveness [4]. There are a number of ways to implement passively mode-locking operation. As well known, nonlinear amplifying/non-amplifying loop mirrors [5],

[6] and nonlinear polarization rotation (NPR) [7], [8] are very common mode-locked techniques. However, the environmental factors such as temperature can affect the stability of the passively mode-locking operation. The physical saturable absorbers (SAs) including semiconductor saturable mirror (SESAM) [9], [10], carbon nanotubes (CNTs) [11]-[14], and graphene [15] have been proposed to achieve passive mode locking. Nevertheless, SESAM has clear disadvantages such as complex manufacture process, limited operation bandwidth, low damage threshold. In contrast, low-dimensional materials such as CNTs and graphene have short recovery times and graphene has broadband response [4], [16]. Nevertheless, graphene and other types of 2D materials-based SA suffering from mass production and quality control issues.

Nowadays, single-walled carbon nanotubes (SWCNTs) still prove to be a type of efficient SAs to realize mode locking due to the short recovery time (~1 ps), low saturation light intensity, and the possibility of mass production. Since the technology was demonstrated in mode-locked fiber lasers firstly [17], many approaches have been developed to fabricate SWCNT-SAs such as direct deposition [18], evanescent field interaction [19], solution [20], dry transfer technique [21], [22], and composite film [12]-[14], [17], [23]. Although the method of fiber end deposition is simple, it is prone to uneven surface deposition and introduces large loss. For the SA type of evanescent field interaction, it is necessary to synthesize the SWCNTs onto the tapered or D-shaped fibers, which requires excessive dependency on the particular fiber structure. And solution-based SWCNT absorbers require hollow fiber with suitable

Manuscript received XXXXXX. This work was supported by the National Natural Science Foundation of China (NSFC) (61605107,61505244), the project was supported by Open Fund of IPOC2017B010 (BUPT), the Open Fund of Key Laboratory of Opto-electronic Information Technology, Ministry of Education (Tianjin University, China) (2018KFKT009), Young Eastern Scholar Program at Shanghai Institutions of Higher Learning (QD2015027); "Young 1000 Talent Plan" Program of China, RAEng and the Leverhulme Trust Senior Research Fellowships (LTSRF1617/13/57), Marie Skłodowska-Curie IEF project (H2020-MSCA-IF-2014\_ST, Proposal#: 656984); Marie-Curie Inter-national Research Staff Exchange Scheme "TelaSens" project, Research Executive Agency Grant No. 269271, Programme: FP7-PEOPLE-2010-IRSES and support from the Ministry of Higher Education, Sultanate of Oman.

Bingbing Lu, Chuanhang Zou, Qianqian Huang and Chengbo Mou are with The Key Lab of Specialty Fiber Optics and Optical Access Network, Shanghai Institute for Advanced Communication and Data Science, Joint International Research Laboratory of Specialty Fiber Optics and Advanced Communication,

Shanghai University, Shanghai, 200444 P. R. China (e-mails: [blany@shu.edu.cn](mailto:blany@shu.edu.cn), [chuanhangzou@i.shu.edu.cn](mailto:chuanhangzou@i.shu.edu.cn); [cecilin@i.shu.edu.cn](mailto:cecilin@i.shu.edu.cn); corresponding author [moucl@shu.edu.cn](mailto:moucl@shu.edu.cn)).

Zhijun Yan and Zhikun Xing are with School of Optical and Electronic Information, National Engineering Laboratory for Next Generation Internet Access System, Huazhong University of Science and Technologies, Wuhan, 430074 P. R. China (e-mail: [yanzhijun@hust.edu.cn](mailto:yanzhijun@hust.edu.cn); [xingzhikun@hust.edu.cn](mailto:xingzhikun@hust.edu.cn)).

Kaiming Zhou, Lin Zhang and Aleksey Rozhin are with Aston Institute of Photonic Technologies (AIPT), Aston University, Birmingham, B4 7ET, United Kingdom (e-mail: [k.zhou@aston.ac.uk](mailto:k.zhou@aston.ac.uk); [L.zhang@aston.ac.uk](mailto:L.zhang@aston.ac.uk); [a.rozhin@aston.ac.uk](mailto:a.rozhin@aston.ac.uk)).

Mohammed Al Araimi is with the Higher College of Technology, Al-Khuwari, PO Box 74, Sultanate of Oman. (email: [malaraimi@gmail.com](mailto:malaraimi@gmail.com))

Color versions of one or more of the figures in this paper are available online at <http://ieeexplore.ieee.org>

Digital Object Identifier xxxxxxxxxxxx

reflective index and low optical loss, which is also complicated to realize. Up to now, the most popular approach to integrate SWCNT-SAs is to sandwich a SWCNT polymer composite film between two fiber connectors. Although it may subject to low damage threshold, the method is promising since the composite film shows excellent homogeneous dispersion of SWCNTs and the physical parameters are much controllable [24].

There are various approaches to achieve wavelength-tuning in mode-locked fiber laser. For example, a micro-mechanically controlled Fabry-Perot interferometer was employed in mode-locked fiber laser [25]. Commercial band-pass filter was demonstrated to realize tunable fiber laser. Li *et al.* have achieved the tuning range of 34 nm and pulse duration changes from 545 fs to 6.1 ps by using a tunable filter [26]. Yet, the band-pass filter has the limited bandwidth and introduce large insertion loss. A better way is based on fiber Bragg grating. He *et al.* have reported a graphene based mode-locked fiber laser with the tuning range of 4.5 nm and 6.6 nm via controlling chirped fiber Bragg grating [27]. Recently, a special cavity structure of drop-shaped topology composed of dual-fiber optical collimator (DFOC) and diffraction grating was proposed, which allowed implementing the tuning range of 78 nm without adjusting any cavity elements (other than the grating) [28]. In addition, a recent developed cascaded long period grating (LPG) has been demonstrated to acquire the wider tuning range of 44 nm by changing the temperature from 23 °C to 100 °C [29]. However, such filter mechanism is difficult to fabricate and unstable. Besides, since the limited tuning range depends on the gain profile of the laser gain medium, Meng *et al.* presented an Er: Yb-doped doubled-clad fiber laser with a wide tuning range of 75 nm by adjusting polarization controllers (PCs) [30]. Also, wavelength-tunable fiber laser with NOLM has been reported which achieved the tuning range of 20 nm [31]. Although tunable mode-locked fiber laser can be realized by adding other elements (such as tunable filter or attenuator), extrinsic components make the structure complex and less compact. It is well known that the intracavity fiber birefringence can generate artificial band-pass filter in a ring cavity. For example, in an NPR-based Erbium-doped mode-locked fiber laser, 38 nm tuning range has been obtained due to the invisible fiber birefringent filtering effect and the total cavity length is 37.4 m [32]. Due to the weak intracavity birefringence, it is necessary to increase the length of SMF to form an effective birefringence filter. However, the total cavity length can be shortened by inserting a polarization maintaining (PM) fiber with strong birefringence. Thus the fundamental repetition rate of the tunable mode locked fiber laser could be elevated which would be useful in many applications. Furthermore, a shorter laser cavity may feature characteristics such as low loss and easy integration. Zhang *et al.* have demonstrated an Ytterbium-doped mode-locked fiber laser with tuning range of 16.7 nm, where a PM fiber with the length of 17.1 cm is used [33]. In a ring fiber laser, polarizer is an indispensable part to form the artificial birefringent band-pass filter. And in-fiber polarizer has many advantages such as high coupling efficiency, low insertion loss, and light weight,

compared with bulk polarizer. Recently, the 45° tilted fiber grating (45°-TFG) with strong polarization dependent loss (PDL), also known as Brewster fiber grating, was employed in the ring all-fiber laser structure as an in-fiber polarizing component. Based on the well-known Brewster effect, the 45°-TFG is a type of fiber grating device that possesses the unique characteristics of lossy *s*-light allowing highly polarized *p*-light to propagate [34].

In this paper, we demonstrate a short cavity wavelength-tunable all-fiber mode-locked Erbium-doped laser based on engineered intracavity fiber birefringence. The cavity length is 8.28 m with a wide tuning range of 36 nm, which is the shortest cavity to acquire such wide tuning range of wavelength. This cavity achieves mode-locked operation through employing SWCNTs-PVA composite film as SA. The collaborative operation of PM fiber and 45°-TFG forms a fiber birefringence filter. When different lengths of PM fiber are inserted into the cavity, the fluctuation of the corresponding tuning range is found to be tiny. Also, the cavity can achieve spectral width and pulse duration tuning upon the birefringent filter. By changing the length of PM fiber, it is also found that the largest variation of spectral width is 5.19 nm when the intracavity PM fiber is set to be 12 cm. Such fiber laser with flexible output performance may found applications in many fields.

## II. FABRICATION AND CHARACTERISTICS OF CNT-SA

A passively Erbium-doped mode-locked fiber laser with stable pulse output can be implemented by using a SWCNTs-PVA composite film as SA. Generally, we fabricate SWCNTs-PVA film with the features of commercially available and purified by using high-pressure CO conversion. For the preparation of SWCNTs-PVA composite film, we can divide it into three steps. Firstly, the SWCNTs of 2 mg are added into 10 ml deionized water mixing with 10 mg sodium dodecylbenzene sulfonate surfactant. Later, a commercial ultrasonicator (Nanoruptor, Diagenode) is used to process the mixed dispersion for sonic degradation with one hour under 200W and 20KHz. The second step is to ultracentrifuge the resulting dispersion at 25000 rpm with one hour using an Optima Max-XP ultracentrifuge (Beckman Coulter). Finally, the dispersion mixing up the PVA powder is set in a Petri dish. And we can acquire the SWCNTs-PVA film by placing the sample in the desiccator for a couple of days until it is fully dried.

The measured linear optical absorption spectrum of the SWCNTs-PVA composite film is shown in Fig.1(a). Due to the transition between the SWCNTs bands, the spectrum features typical three main absorption bands  $E_{11}$ ,  $E_{22}$ , and  $M_{11}$  separately. The obtained optical spectrum displays an optical density of 0.17 near the absorption wavelength of 1550 nm, which matches the lasing wavelength of Erbium-doped fiber lasers. The measured Raman spectrum of the SWCNTs-PVA SA with an excitation wavelength of 532 nm is depicted in Fig. 1(b). The radial breathing modes (RBMs, 150-300  $\text{cm}^{-1}$ ), the disorder mode (D,  $\sim 1350 \text{ cm}^{-1}$ ) and graphite mode (G,  $\sim 1590 \text{ cm}^{-1}$ ) are the crucial characteristics in the Raman spectrum of SWCNTs. The obtained spectrum for SWCNTs-PVA composite film displays a strong peak at 272  $\text{cm}^{-1}$ . The average nanotube

diameter is calculated to be 0.89 nm because the RBM is related to the diameter [35]. Furthermore, the obtained Raman spectrum presents strong G peak and an insignificant increase in the D peak. This indicates that SWCNTs' preparation does not alter the electronic properties of the source materials. Fig. 1(c) shows the measured nonlinear transmission. The modulation depth can be estimated as about 3.0%, which further proves that the SWCNTs-PVA film can be used as an ideal mode-locked element.

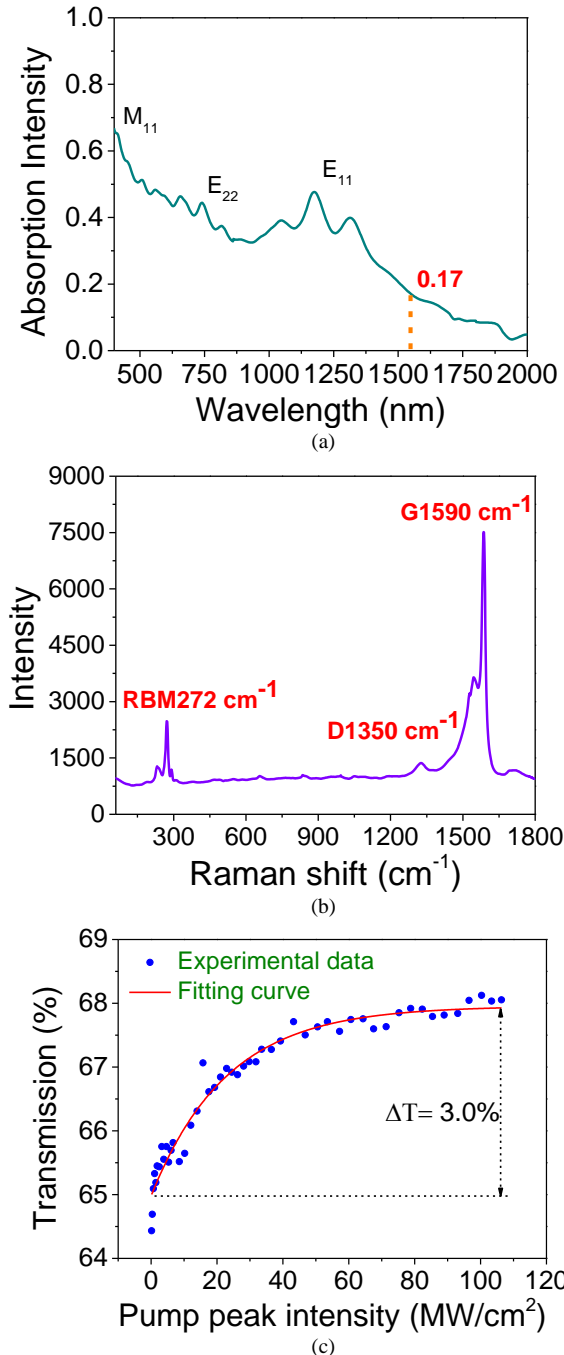


Fig. 1. (a) Absorption spectrum of the SWCNTs-PVA film, (b) the measured Raman spectrum of the SWCNTs-PVA film, (c) nonlinear transmission of the SWCNTs-PVA film.

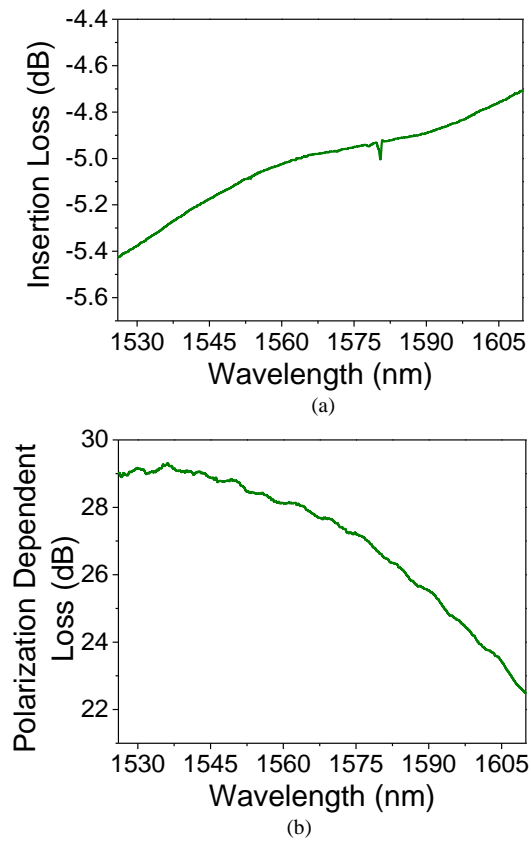


Fig. 2. (a) The transmission spectrum of the 45°-TFG, (b) the PDL response of the 45°-TFG.

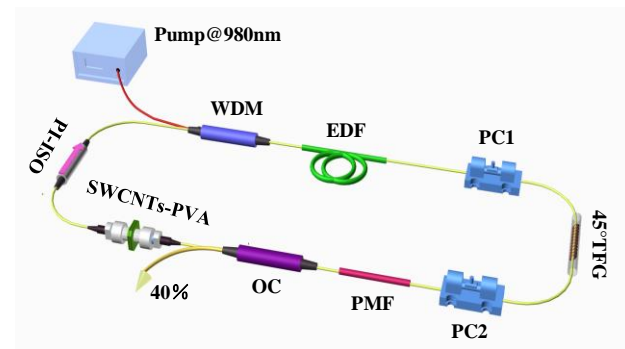


Fig. 3. Schematic of the tunable fiber laser.

### III. CHARACTERISTICS OF 45°-TFG

The 45°-TFG is UV inscribed in a commercial single mode fiber by the standard phase mask scanning technique. The fabrication process can be found elsewhere in ref [36]. The 45°-TFG exhibits a strong PDL owing to the Brewster law [37]. We measure the PDL response using a commercial optical vector analyzer (from LUNA system). The measured transmission spectrum from 1526 nm to 1610 nm is shown in Fig. 2(a). The insertion loss is -5.1 dB at 1550nm, which includes the loss induced by *s*-light coupled into cladding and other loss due to the non-ideal connection and splicing. Fig. 2(b) shows that the 45°-TFG has a strong PDL of 29 dB at 1550 nm.

### IV. EXPERIMENT SETUP AND PRINCIPLE

The schematic of the laser cavity is shown in Fig. 3. A section

of 1.08 m highly doped Erbium fiber (EDF Er80-8/125 from Liekki) whose nominal dispersion is  $-20 \text{ ps}^2/\text{km}$ , serves as the gain medium in the cavity. It is pumped by a benchtop 980 nm laser module (OV LINK) through a 980/1550 nm wavelength division multiplexer (WDM) whose pigtail is 2.47 m OFS980 fiber with  $+4.5 \text{ ps}^2/\text{km}$  normal dispersion. After that, a  $45^\circ$ -TFG is inserted between two PCs. The purpose of using two in-line PCs in the proposed laser scheme is just simply to make sure that a broader range of polarization state would be covered. The function of PM fiber is to enhance intracavity birefringent effect, so as to realize the parameter tuning of output pulse by combining with the  $45^\circ$ -TFG. And they are necessary to obtain the wavelength tuning mechanism. The unidirectional operation is maintained by the polarization independent isolator (PI-ISO). The SWCNTs-PVA composite film is clipped between two fiber connectors to provide self-starting mode locking. The cavity extracts out 40% energy via a 40/60 optical coupler for signal detection. The laser output optical spectra are monitored by an optical spectrum analyzer (OSA, Yokogawa AQ6370C). The pulse train are studied by high speed oscilloscope (KEYSIGHT DSO90804A) with a fast detector (Newport 818-BB-51F, 12GHz). The pulse stability is studied by a radio frequency analyzer (SSA, 3032X). And the pulse width is analyzed by using a commercial autocorrelator (FEMTOCHROME, FR-103WS).

The transmission modulation function of intracavity

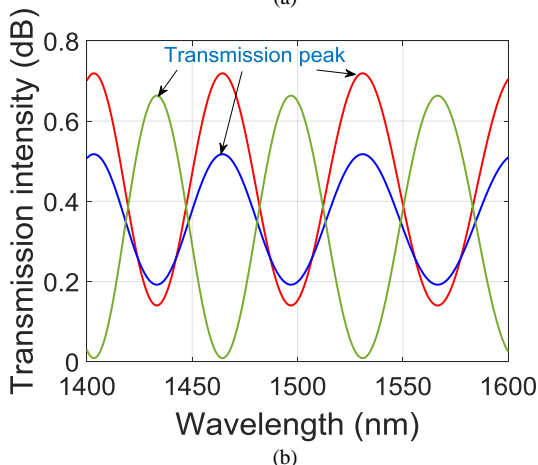
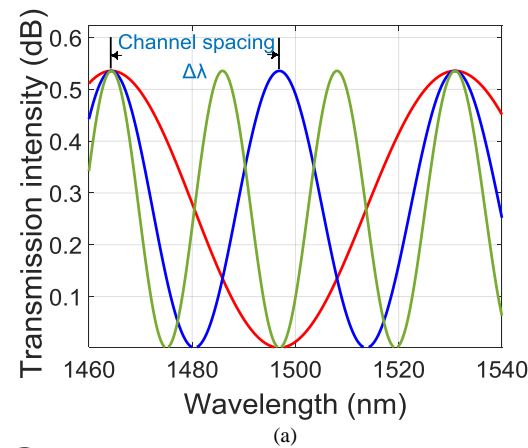


Fig. 4. Calculated tunable transmission spectra of changing (a) the length of PM fiber and (b) the angle by rotating the PCs.

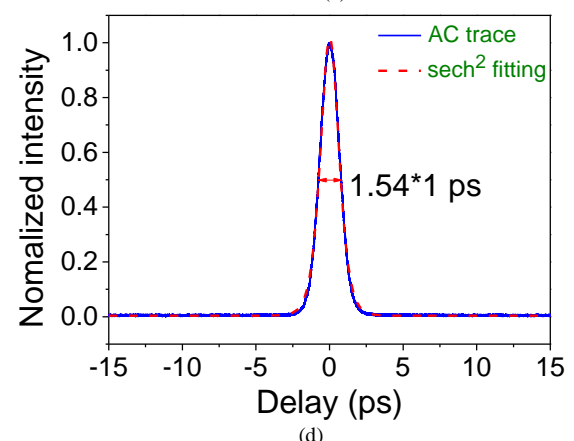
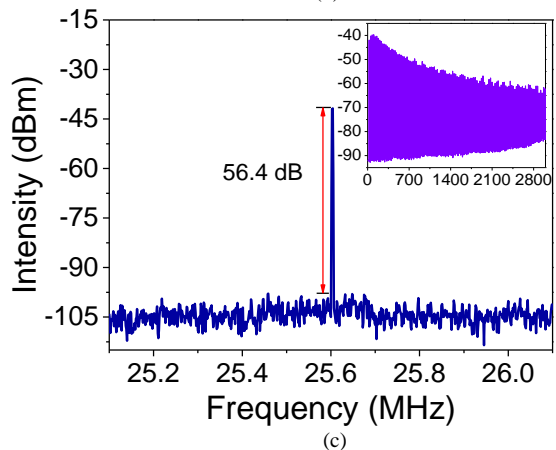
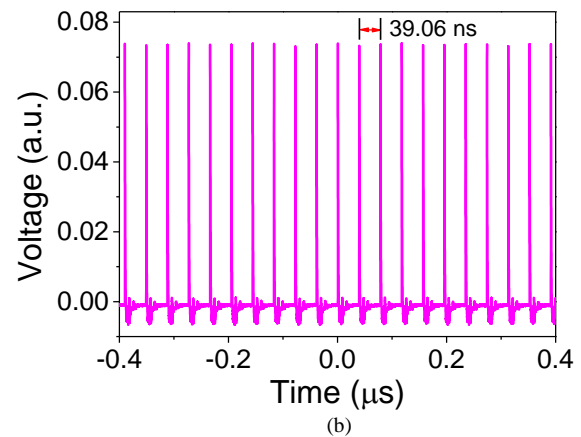
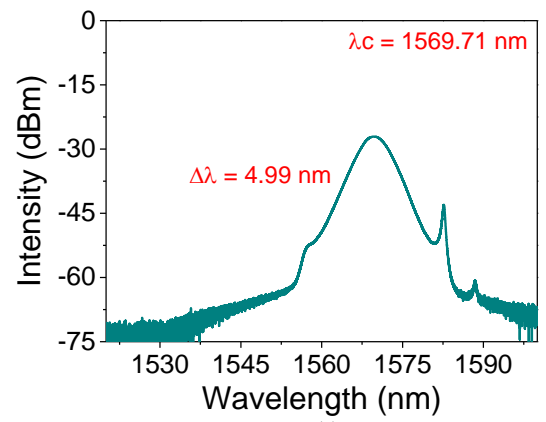


Fig. 5. (a) Optical spectrum, (b) oscilloscope trace, (c) the RF spectrum, (d) autocorrelation trace of the pulse.

birefringence-induced filter can be described as [38], [39]:

$$T = \cos^2 \alpha \cos^2 \beta + \sin^2 \alpha \sin^2 \beta + \frac{1}{2} \sin(2\alpha) \sin(2\beta) \cos(\Delta\varphi_L + \Delta\varphi_{NL})$$

In this formula,  $\alpha$  and  $\beta$  are defined as the angles between the polarization directions of the 45°-TFG and the fast axis of the fiber.  $\Delta\varphi_L$  is the linear cavity phase shift, expressed as  $\Delta\varphi_L = 2\pi L(n_y - n_x)/\lambda$ , and  $\Delta\varphi_{NL}$  is the nonlinear cavity phase shift, which is given by  $\Delta\varphi_{NL} = 2\pi n_2 P L \cos(2\alpha)/(\lambda A_{eff})$ . Here,  $L$  represents the length of PM fiber,  $n_2$  is the nonlinear coefficient,  $\lambda$  is the operating wavelength,  $P$  is the peak power of the input signal and  $A_{eff}$  is the effective mode field. It is well known that the transmission channel spacing  $\Delta\lambda$  can be described as  $\Delta\lambda = \lambda^2/(n_y - n_x)L$ , which is related to the birefringence and the PM fiber length. Hence, the transmission channel spacing will be changed when we set PM fiber to different lengths. The three transmission curves are drawn with PM fibers of 8 cm (red line), 16 cm (blue line), and 24 cm (green line), respectively, as shown in Fig. 4(a). Moreover, the transmission peak position depends on the value of  $\alpha$  and  $\beta$ , which can be tuned by rotating the PC. Thus, the wavelength-tunable mode-locked pulse can be achieved by rotating the PC properly. In the simulation, three sets of angles are taken when the length of PM fiber is fixed to 8 cm, and the birefringence is  $4.21 \times 10^{-4}$ . The three curves are drawn out with parameters of  $\alpha=7\pi/9$  and  $\beta=3\pi/5$  (red line),  $\alpha=6\pi/5$  and  $\beta=4\pi/9$  (blue line),  $\alpha=25\pi/22$  and  $\beta=11\pi/3$  (green line) in Fig. 4(b).

## V. EXPERIMENT RESULTS

Firstly, an 8-cm-long PM fiber with the birefringence  $\Delta n$  of  $4.21 \times 10^{-4}$  is placed in the fiber laser. The total cavity length is 8.28 m. It is calculated that the net dispersion of the cavity is  $-0.12 \text{ ps}^2$ , which indicates the passively mode-locked fiber laser operates in net anomalous dispersion regime. When the pump power reaches 200 mW, stable mode-locked pulses can be observed. Generally, the mode-locked operation based on NPR requires high pump power. The fiber laser realizes mode locking only by CNT-SA since the pump power is not enough to achieve NPR-based mode locking. The view is verified by the experimental phenomenon in which removing the SWCNT composite film failed to achieve passive mode locking. Fig. 5(a) shows the typical output optical spectrum of the mode-locked pulse with the 3dB bandwidth of 4.99 nm centered at 1569.71 nm. The existence of the Kelly sideband proves that the fiber laser works in conventional soliton regime. The corresponding pulse train is shown in Fig. 5(b) indicating that the pulse interval is 39.06 ns. Fig. 5(c) is the measured RF spectrum showing a fundamental repetition rate of 25.6 MHz with the resolution bandwidth (RBW) of 1 kHz. And the signal to noise ratio (SNR) of 56.4 dB indicates that the laser operates in a stable state. The inset in Fig. 5(c) shows the RF spectrum from 0 to 3 GHz with the RBW of 10 kHz. Fig. 5(d) exhibits the autocorrelation trace. The pulse duration is estimated to be  $\sim 1 \text{ ps}$  when it is well-fitted to a  $\text{sech}^2$  temporal profile. Thus, the time-bandwidth product (TBP) is 0.64, showing that the pulse is slightly chirped. As discussed in the simulation above, the mode-locked pulse can

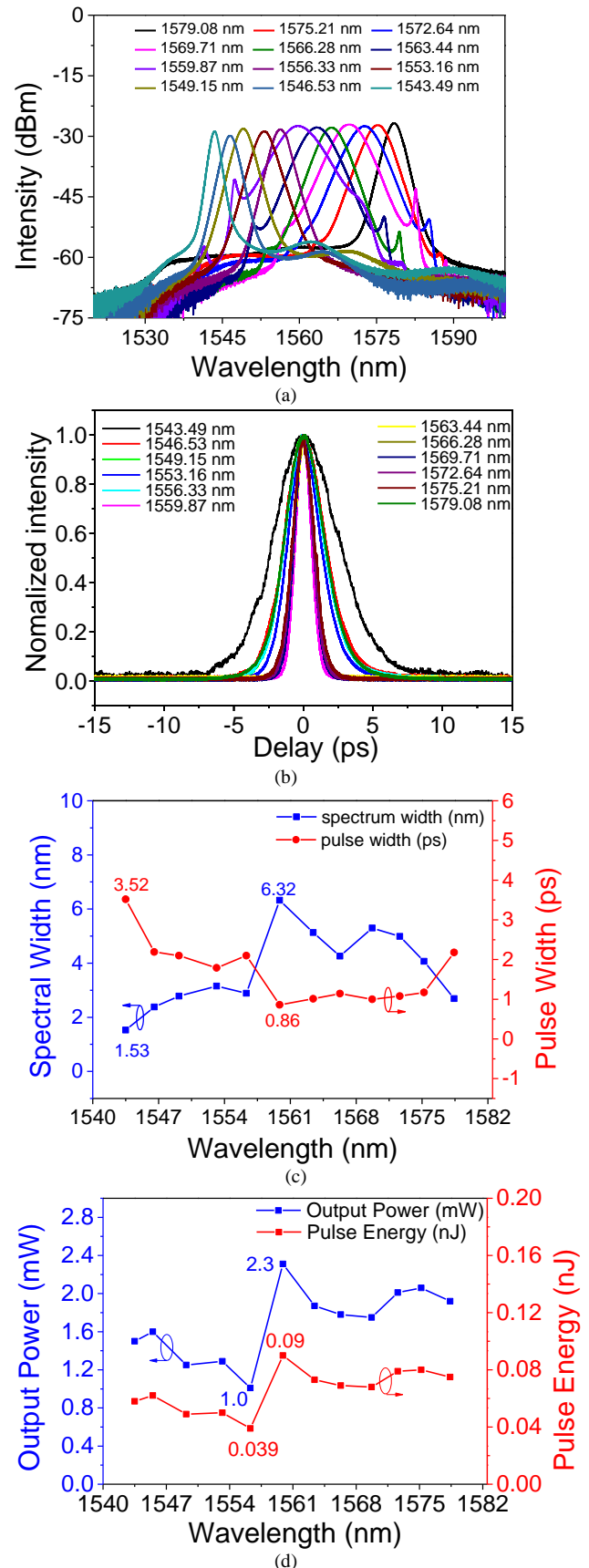


Figure 6. Typical tuning characteristics of the fiber laser with 8 cm PM fiber. (a) Measured spectral tunability of mode-locked fiber laser, (b) autocorrelation traces of output pulses at different central wavelength, (c) the variation of 3 dB bandwidth and pulse width, (d) the variation of output power and single pulse energy.



be tuned by rotating two PCs properly. It can be seen in Fig. 6(a) that the fiber laser obtains the wavelength tunable range of 36 nm from 1543.49 to 1579.08 nm. In the wavelength domain, the total cavity net dispersion changes slightly. And the shape of optical spectra shows minor variation at different central wavelength. In particular, the Kelly sideband are not manifested at some wavelength. This is because the transmission bandwidth of the birefringence filter is variable by adjusting the PCs. The Kelly sideband would be filtered out when the filter bandwidth is narrow enough. Fig. 6(b) shows the corresponding autocorrelation traces at different central wavelengths. The pulse width changes from 0.86 to 3.52 ps, and the corresponding spectral width varies from 6.32 to 1.53 nm, as shown in Fig. 6(c). Therefore, we can clearly see that the pulse width and spectral width change obviously. This is simply because of the birefringent filter defined spectral transmission variation. From Fig. 6(d), we can observe that the output power changes from 1 to 2.3 mW while the pump power remains

mode locked laser system. The laser output power variation range is between ~1 mW and ~3 mW. The pulse energy variation is between ~0.03 nJ and ~0.1 nJ. Note that, in the experiment, we have not explored the pulse properties with increased pump power. This is simply because of the well-known low thermal damage threshold of CNT polymer composite SA. The avoidance of multiple pulsing and SA damage were considered.

In the simulation, the transmission channel spacing changes depending on the PM fiber length. To further investigate the influence of PM fiber length variation on the spectral tuning range experimentally, the lengths of PM fibers are set to be 8 cm, 12 cm, 16 cm, 20 cm, 24 cm separately. As stated in Table I, the corresponding spectral tuning ranges are 36, 36, 32, 30, and 30 nm, respectively. Note that the maximum and minimum spectral tuning range achieved with different lengths of PM fiber differ only by 6 nm. Thus, the length of PM fiber has small influence on the tuning range realized by mode-locked fiber laser. It is because the spectral tuning range is mainly determined by the gain of the EDF [3], [40].

As mentioned above, both pulse width and spectral width are also tunable as the central wavelength of the output pulse changes. From Fig. 7, we can observe that the realized tuning range of the spectral width is subjected to the length of the cavity inserted PM fibers. Among these, the variation of spectral width reaches the maximum of 5.19 nm when the PM fiber is 12-cm long. According to the formula,  $\Delta\lambda$  is inversely proportional to the length of PM fiber. Thence, the channel spacing is smaller with the longer length of PM fiber, which is not conducive to spectral broadening. However, the shorter PM fiber results in a large bandwidth of the filter, so that the filter effect is not obvious. Therefore, the 3dB bandwidth of the spectrum can be obtained with a large variation range, when the length of PM fiber is appropriate. Note that, for all PM fiber lengths, the 3 dB bandwidths of the optical spectra with central wavelength at 1560 nm are around 6 nm. Besides, the tuning ranges of pulse width are almost approximative under different lengths of PM fiber, as shown in Fig. 7. The pulse width changes from 0.86 to 3.52 ps (from 0.83 to 2.77 ps, from 1.05 to 2.81 ps, from 0.87 to 3.50 ps, and from 1.02 to 3.43 ps) corresponding to the PM fiber length of 8 cm (12 cm, 16 cm, 20 cm, and 24 cm). We calculate the TBPs of the soliton pulses are around 0.7, which indicates that the output pulses are chirped. It is mainly due to the existence of the OFS980 fiber with +4.5ps<sup>2</sup>/km normal dispersion. The TBPs of the pulses may be close to the transform-limited value by adjusting the length of the SMF outside the cavity properly. Moreover, the measured SNR of the pulses at the boundary of the implemented spectral tuning range are 43 dB approximately, and the SNR of the remaining pulses are about 54 dB. This is owing to the lower gain of the pulses at the boundary of the spectral tuning range. Thus, the proposed fiber laser has stable output mode-locking pulses.

In addition, we evaluate the tunability of the mode-locked fiber laser without PM fiber by adjusting the PCs. The fiber laser achieves the tuning range of 24 nm. The central wavelength changes from 1550.22 to 1574.09 nm. Therefore,

TABLE I  
COMPARISON OF WAVELENGTH-TUNABLE RANGES WITH DIFFERENT LENGTHS OF PM FIBER

PM Fiber (cm)	Tuning Range (nm)
8	36
12	36
16	32
20	30
24	30

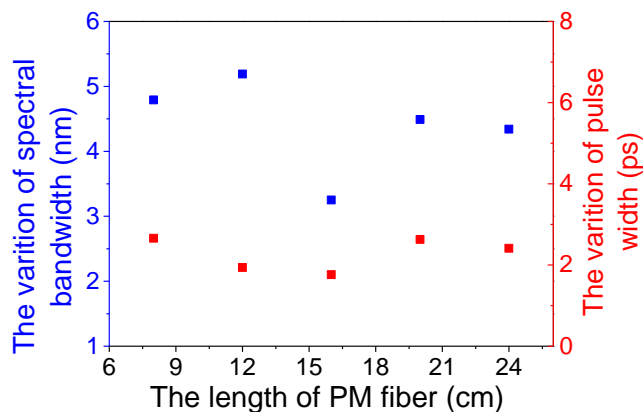


Fig. 7. The variation of spectral width and pulse width against intracavity PM fiber length.

constant. By calculation, the corresponding pulse energy changes from 0.039 to 0.09 nJ. Relatively lower output pulse power and energy at the boundary of spectral tuning range is owing to the lower gain compared to the maximum region at ~1560 nm. It turns out that single-pulse energies and cavity loss change slightly against the variation of the central wavelength. The variation of pulse energy and power is obviously a result of the polarization controller induced spectral change with the corresponding transmission alteration. A similar trend in terms of the pulse energy and power has been identified while other length of PM fiber was incorporated in the laser cavity respectively. A maximum output power was found at ~1560 nm which is quite typical in most of the Erbium doped fiber

PM fiber plays an important role to achieve wide tuning range owing to the strong birefringent effect. Such a multi-parameter tunable fiber laser demonstrated in this work provides a new approach to develop novel ultrafast source.

## VI. CONCLUSION

In conclusion, we have reported a wavelength and spectral width tunable all-fiber mode-locked Erbium-doped fiber laser based on PM fiber and 45°-TFG. The cooperative operation of PM fiber and 45°-TFG can form an effective fiber birefringence filter. The wavelength tunable range of 36 nm is obtained with 8 cm PM fiber by rotating two PCs. Also, the cavity length is 8.28 m, which is the shortest cavity length to achieve a mode-locked fiber laser with wide tuning range. We experimentally found that the variation of PM fiber length does not affect the tuning range greatly. Simultaneously, the corresponding spectral width and pulse duration are tunable. For the PM fiber length of 12 cm, the 3 dB spectral width achieves the largest tuning range of 5.19 nm, which changes from 1.89 to 7.08 nm with a corresponding pulse duration from 0.83 to 2.77 ps. Such flexible output wavelength and spectral width tunable fiber laser can be applied in fundamental research and commercial applications, such as spectroscopy, laser processing and optical communication. We also expect our study may provide useful guidance in designing parameter tunable mode locked fiber lasers.

## REFERENCES

- [1] N. K. Chen, J. W. Lin, F. Z. Liu, and S. K. Liaw, "Wavelength-Tunable Er<sup>3+</sup>-Doped fs Mode-Locked Fiber Laser Using Short-Pass Edge Filters," *IEEE Photonics Technol. Lett.*, vol. 22, no. 10, pp. 700-702, May. 2010.
- [2] X. H. Li et al, "Wavelength-Switchable and Wavelength-Tunable All-Normal-Dispersion Mode-Locked Yb-Doped Fiber Laser Based on Single-Walled Carbon Nanotube Wall Paper Absorber," *IEEE Photonics J.*, vol. 4, no. 1, pp. 234-241, Feb. 2012.
- [3] H. Zhang, D. Y. Tang, R. J. Knize, L. M. Zhao, Q. L. Bao, and K. P. Loh, "Graphene mode locked, wavelength-tunable, dissipative soliton fiber laser," *Appl. Phys. Lett.*, vol. 96, no. 11, pp. 111-112, Mar. 2010.
- [4] J. H., S. Y. Choi, F. Rotermund, K. Lee, and D. Yeom, "All-polarization maintaining passively mode-locked fiber laser using evanescent field interaction with single-walled carbon nanotube saturable absorber," *J. Lightwave Technol.*, vol. 34, no. 15, pp. 3510-3514, Aug. 2016.
- [5] M. E. Fermann, F. Haberl, M. Hofer, and H. Hochreiter, "Nonlinear amplifying loop mirror," *Opt. Lett.*, vol. 15, no. 13, pp. 752-754, Jul. 1990.
- [6] N. J. Doran, and D. Wood, "Nonlinear-optical loop mirror," *Opt. Lett.*, vol. 13, no. 1, pp. 56-58, Jan. 1988.
- [7] Z. X. Zhang, L. Zhan, K. Xu, J. Wu, Y. X. Xia, and J. T. Lin, "Multiwavelength fiber laser with fine adjustment, based on nonlinear polarization rotation and birefringence fiber filter," *Opt. Lett.*, vol. 33, no. 4, pp. 324-326, Feb. 2008.
- [8] Z. C. Luo, A. P. Luo, W. C. Xu, C. X. Song, Y. X. Gao, and W. C. Chen, "Sideband controllable soliton all-fiber ring laser passively mode-locked by nonlinear polarization rotation," *Laser Phys. Lett.*, vol. 6, no. 8, pp. 582-585, April. 2009.
- [9] U. Keller, "Recent developments in compact ultrafast lasers," *Nat.*, vol. 424, pp. 831-838, Aug. 2003.
- [10] G. Lin, W. Hou, H. B. Zhang, Z. P. Sun, D. Cui, and Z. Y. Xu, "Diode-end-pumped passively mode-locked ceramic Nd: YAG Laser with a semiconductor saturable mirror," *Opt. Express*, vol. 13, no. 11, pp. 4085-4089, May. 2005.
- [11] E. J. R. Kelleher, J. C. Travers, Z. Sun, A. G. Rozhin, A. C. Ferrari, S. V. Popov, and J. R. Taylor, "Nanosecond-pulse fiber lasers mode-locked with nanotubes," *Appl. Phys. Lett.*, vol. 95, no. 11, pp. 111108-3, Sep. 2009.
- [12] S. Kivistö et al., "Carbon nanotube films for ultrafast broadband technology," *Opt. Express*, vol. 17, no. 4, pp. 2358-2363, Feb. 2009.
- [13] X. Liu, D. Han, Z. P. Sun, C. Zeng, H. Lu, D. Mao, Y. D. Cui, and F. Q. Wang, "Versatile multi-wavelength ultrafast fiber laser mode-locked by carbon nanotubes," *Sci. Rep.*, Sep. 2013.
- [14] Z. H. Yu, Y. G. Wang, X. Zhang, X. Z. Dong, J. R. Tian, and Y. R. Song, "A 66 fs highly stable single wall carbon nanotube mode locked fiber laser," *Laser Phys.*, vol. 24, pp. 015105-5, 2014.
- [15] G. Sobon et al., "Graphene oxide vs. reduced graphene oxide as saturable absorbers for Er-doped passively mode-locked fiber laser," *Opt. Express*, vol. 20, no. 17, pp. 19463-19473, Aug. 2012.
- [16] A. Martinez, Z. P. Sun, "Nanotube and graphene saturable absorbers for fiber lasers," *Nat. Photonics*, vol. 7, no. 11, pp. 842-845, Nov. 2013.
- [17] S. Y. Set, H. Yaguchi, Y. Tanaka, and M. Jablonski, "Mode-locked fiber lasers based on a saturable absorber incorporating carbon nanotubes," *Optical Fiber Communication Conference, Opt. Soc. Am.*, 2003.
- [18] Y. Sakakibara, S. Tatsuura, H. Kataura, M. Tokumoto, and Y. Achiba, "Near-Infrared Saturable Absorption of Single-Wall Carbon Nanotubes Prepared by Laser Ablation Method," *J. Appl. Phys.*, vol. 42, no.5A, pp. L494-L496, May. 2003.
- [19] Y. W. Song, and S. Yamashita, "Carbon nanotube mode lockers with enhanced nonlinearity via evanescent field interaction in D-shaped fibers," *Opt. Lett.*, vol. 32, no. 2, pp. 148-150, Jan. 2007.
- [20] A. Martinez, K. Zhou, T. Bennion, and S. Yamashita, "In-fiber microchannel device filled with a carbon nanotube dispersion for passive mode-lock lasing," *Opt. Express*, vol. 16, no. 20, pp. 15425-15430, Sep. 2008.
- [21] A. Kaskela et al., "Aerosol-synthesized SWCNT networks with tunable conductivity and transparency by a dry transfer technique," *Nano Lett.*, pp. 4349-4355, Oct. 2010.
- [22] S. Kobtsev et al., "Ultrafast all-fiber laser mode-locked by polymer free carbon nanotube film," *Opt. Express*, vol. 24, no. 25, pp. 28768-28773, Dec. 2016.
- [23] M. A. Ismail, S. W. Harun, N. R. Aulkepey, R. M. Nor, F. Ahmad, and H. Ahmad, "Nanosecond soliton pulse generation by mode-locked erbium-doped fiber laser using single-walled carbon-nanotube-based saturable absorber," *Appl. Opt.*, vol. 51, no. 36, pp. 8621-8624, Dec. 2012.
- [24] M. H. M. Ahmed, N. M. Ali, Z. S. Salleh, A. A. Rahman, S. W. Harun, M. Manaf, and H. Arof, "All fiber mode-locked Erbium-doped fiber laser using single-walled carbon nanotubes embedded into polyvinyl alcohol film as saturable absorber," *Opt. Laser Technol.*, vol. 62, pp. 40-43, Mar. 2014.
- [25] J. S. Milne, J. M. Dell, A. J. Keating, and L. Faraone, "Widely tunable MEMS-based Fabry-Perot filter," *J. Microelectromech. Syst.*, vol. 18, no.4, pp. 905-913, Jul. 2009.
- [26] D. Li et al., "Wavelength and pulse duration tunable ultrafast fiber laser mode-locked with carbon nanotubes," *Sci. Rep.*, vol. 8, 2018.
- [27] X. Y. He, Z. B. Lin, and D. N. Wang, "Wavelength-tunable, passively mode-locked fiber laser based on graphene and chirped fiber Bragg grating," *Opt. Lett.*, vol. 37, no. 12, pp. 2394-2396, Jun. 2012.
- [28] B. Nyushkov, S. Kobtsev, A. Antropov, D. Kolker, and V. Pivtsov, "Femtosecond 78-nm tunable Er: fiber laser based on drop-shaped resonator topology," *J. Lightwave Technol.*, vol. 37, no. 4, pp. 1359-1363, Feb. 2019.
- [29] J. Wang, A. P. Zhang, Y. H. Shen, H. Y. Tam, and P. K. Wai, "Widely tunable mode-locked fiber laser using carbon nanotube and LPG W-shaped filter," *Opt. Lett.*, vol. 40, no. 18, pp. 4329-4332, Sep. 2015.
- [30] Y. C. Meng, M. Salhi, A. Niang, K. Guesmi, G. Semaan, and F. Sanchez, "Mode-locked Er:Yb-doped double-clad fiber laser with 75-nm tuning range," *Opt. Lett.*, vol. 40, no. 7, pp. 1153-1156, Apr. 2015.
- [31] X. H. Li et al., "All-normal dispersion, figure-eight, tunable passively mode-locked fiber laser with an invisible and changeable intracavity bandpass filter," *Laser Phys.*, vol. 21, no. 5, pp. 940-944, Apr. 2011.
- [32] Z. R. Cai, W. J. Cao, A. P. Luo, Z. B. Lin, Z. C. Luo, and W. C. Xu, "A wide-band tunable femtosecond pulse fiber laser based on an intracavity-birefringence induced spectral filter," *Laser Phys.*, vol. 23, no.3, 2013.
- [33] Z. X. Zhang, Z. W. Xu, and L. Zhang, "Tunable and switchable dual-wavelength dissipative soliton generation in an all-normal-dispersion Yb-doped fiber laser with birefringence fiber filter," *Opt. Express*, vol. 20, no. 24, pp. 26736-26742, Nov. 2012.
- [34] C. B. Mou, H. Wang, B. G. Bale, K. Zhou, L. Zhang, and I. Bennion, "All-fiber passively mode-locked femtosecond laser using a 45°-tilted fiber grating polarization element," *Opt. Express*, 2010.
- [35] A. Jorio, R. Saito, J. H. Hafner, C. M. Lieber, M. Hunter, T. McClure, et al., "Structural (n, m) determination of isolated single-walled carbon

- nanotubes by resonant Raman scattering,” *Phys. Rev. Lett.*, vol. 86, pp. 1118-21, Feb. 2001.
- [36] Z. J. Yan, C. B. Mou, K. M. Zhou, X. F. Chen, and L. Zhang, “UV-Inscription, Polarization-Dependent Loss Characteristics and Applications of 45° Tilted Fiber Gratings,” *J. Lightwave Technol.*, vol. 29, no. 18, pp. 2715-2724, Sep. 2011.
- [37] C. B. Mou, K. M. Zhou, L. Zhang, and I. Bennion, “Characterization of 45°-tilted fiber grating and its polarization function in fiber ring laser,” *J. Opt. Soc. Am. B*, vol. 26, no. 10, pp. 1905-1911, Oct. 2009.
- [38] C. J. Chen, P. K. A. Wai, and C. R. Menyuk, “Soliton fiber ring laser,” *Opt. Lett.*, vol. 17, no. 6, pp. 417-419, Mar. 1992.
- [39] D. Y. Tang, L. M. Zhao, B. Zhao, and A. Q. Liu, “Mechanism of multisoliton formation and soliton energy quantization in passively mode-locked fiber lasers,” *Phys. Rev. A*, vol. 72, 2005.
- [40] Z. Y. Yan *et al.*, “Widely tunable Tm-doped mode-locked all-fiber laser,” *Sci Rep*, vol. 6, 2016.

**Bingbing Lu** was born in Shangqiu, Henan, China, in 1994. She received the B.S. degree from North China University of Water Resources and Electric Power, Henan, China, in 2017. And she is currently working towards the M. Eng. degree at the Key Lab of Specialty Fiber Optics and Optical Access Network, Shanghai University, Shanghai, in 2017. Her current research focus is on wavelength-tunable passively mode-locked fiber laser.

**Chuanhang Zou** was born in Hangzhou, Zhejiang, China, in 1992. He received the B.S. degree from Tianjin University of Technology, Tianjin, China, in 2016. And he is currently working towards the M. Eng. degree at the Key Lab of Specialty Fiber Optics and Optical Access Network, Shanghai University, Shanghai, in 2016. His current research focus is on wavelength-tunable passively mode-locked fiber laser.

**Qianqian Huang** was born in Wenzhou, Zhejiang, China, in 1993. She received the B.S. degree from Zhejiang Science and Technology University, Zhejiang, China, in 2016. And she is currently working towards the M. Eng. degree at the Key Lab of Specialty Fiber Optics and Optical Access Network, Shanghai University, Shanghai, in 2016. Her current research focus is on high repetition rate fiber laser and nonlinear fiber optics.

**Zhijun Yan** received the B.Sc. and M.Sc. degrees in physics from Lanzhou University, Lanzhou, China, in 2003 and 2005, respectively, and the Ph.D. in photonics from the Aston Institute of Photonic Technologies, Aston University, Birmingham, U.K., in 2013. He worked as a Research Fellow with Aston University in advanced fiber grating sensors for three years. In 2016, he joined Huazhong University of Science and Technology, Wuhan, China. He has extensive experience in fabricating, characterizing specialty fiber grating devices. He has also developed a couple of novel fiber grating applications including side tapped detection method in biological study. His major research interests include specialty fiber grating devices and their applications in advanced sensing, imaging, fiber lasers, and metrology.

**Aleksey Rozhin** received the M.S. degree in physics from Taras Shevchenko National University of Kiev, Kiev, Ukraine, in 1998, and the Ph.D. degree in solid state physics from the Institute for Semiconductor Physics, National Academy of Science of Ukraine, Kiev, Ukraine, in 2001. From 2001 to 2002, he was a Researcher with the Institute for Semiconductor

Physics NASU, Ukraine. From 2002 to 2005, he was JSPS, AIST Postdoctoral Fellow with the National Institute of Advanced Industrial Science and Technology, Japan. From 2005 to 2009, he was a Senior Research Associate with the Centre for Advanced Photonics and Electronics, University of Cambridge, U.K. Since 2009, he has been with Aston University, Birmingham, U.K., first as a Lecturer, where he became a Senior Lecturer in 2012, in Nanotechnology. His current research interests include nanomaterials synthesis, nanomaterials surface functionalization, development of nanocomposites for photonic applications, solid-state physics, and biophysics. He is working on designing and developing novel ultrafast lasers, polymer waveguides, optical switches, signal regenerative filters, fibre and waveguide sensors, microfluidic devices. He has published more than 60 journal and ten conference papers in the area of photonics and nonlinear optical materials, fibre lasers, fibre communication devices, and filed ten patent applications.

**Kaiming Zhou** received the Ph.D. degree from the Institute of Semiconductors, Chinese Academy of Sciences, Beijing, China, in 1999. He joined Aston University, Birmingham, U.K., in 2002. His research interests include photonic device physics, fiber gratings, fiber optical sensors, fiber laser and semiconductor lasers, and laser microfabrication of photonic devices. He has authored and coauthored more than 100 publications in high-standard international journals and conferences.

**Lin Zhang** is currently a Professor with the Aston Institute of Photonic Technologies, Aston University, Birmingham, U.K. She is also the Head of Electrical, Electronic and Power Engineering, Aston University. Her research interests include optical fiber grating devices and their applications in optical communications, signal processing, bio-photonics, fiber lasers, and smart sensing. Her research output so far includes ~430 research papers published in peer-review journals and international conferences.

**Chengbo Mou** received the B.Eng. degree in electronic science and technologies from Tianjin University, Tianjin, China, in 2004, the M.Sc. degree in photonics and optoelectronic devices from the University of St Andrews, St Andrews, U.K., in 2005, the Ph.D. degree in photonics from the Aston Institute of Photonic Technologies, Aston University, Birmingham, U.K., in 2012. He then worked as an Industrial Research Fellow with Aston University. In 2016, he joined in the Key Laboratory of Specialty Fiber Optics and Optical Access Networks as a Full Professor. His research interests include nanophotonics, nanomaterial-based nonlinear photonic devices, ultrafast fiber lasers, novel type of mode locked lasers, and nonlinear applications of advanced fiber grating devices. He is the recipient of National “Young 1000 Talent” programme of China, the Young Eastern Scholar Fellowship from the Shanghai Institute of Higher Learning.